900 *Inorg. Chem.* **2011**, *50*, 900–910
DOI: 10.1021/ic101467s

Inorganic Chemistry
Article

Heteroscorpionate-Based Co^{2+}, Zn^{2+}, and Cu^{2+} Complexes: Coordination Behavior, Aerobic Oxidation, and Hydrogen Sulfide Detection

Maria Strianese, Stefano Milione,* Valerio Bertolasi,† Claudio Pellecchia, and Alfonso Grassi

Dipartimento di Chimica, Università di Salerno, via Ponte don Melillo, I-84084 Fisciano (SA), Italy.
† Università di Ferrara, Centro di Strutturistica Diffrattometrica e Dipartimento di Chimica, Via L. Borsari, 46, I-44100 Ferrara, Italy

Received July 22, 2010

The coordination behavior and reactivity of the phenol-substituted bis(pyrazolyl)methane ligands, (3,5-^{t}Bu$_2$-2-phenol)-bis(3,5-Me$_2$-pyrazol-1-yl)methane (*L1*-H) and 2-phenol-bis(3,5-Me$_2$-pyrazol-1-yl)methane (*L2*-H) have been investigated in the metal complexes (*L1*-H)$CoCl_2$ (**1**), (*L1*-H)$ZnCl_2$ (**2**), (*L3*)$CuCl_2$ (**3**), (*L2*)$_2Co_2Cl_2$ (**4**) (*L2*-H)$ZnCl_2$ (**5**), and (*L2*-H)$CuCl_2 \cdot H_2O$ (**6**). The mononuclear tetrahedral cobalt complex **1** was isolated and fully characterized by X-ray single crystal diffraction and ^{1}H NMR spectroscopy and relaxometry. The neutral *L1*-H is κ^2-coordinated to the metal center whereas the not coordinated hydroxy-phenyl group is involved in extended intermolecular hydrogen bonds. Aerobic oxidation of *L1*-H was observed in the reaction of this ligand with $CuCl_2$ to yield the *para*-quinone derivative *L3* (*L3* = 2-^{t}Bu-6-(bis(3,5-Me$_2$-pyrazol-1-yl)methyl)cyclohexa-2,5-diene-1,4-dione). Upon oxidation *L3* resulted κ^2-coordinated to the tetrahedral Cu(II) metal center, affording **3**. The reaction of *L2*-H with $CoCl_2 \cdot 6H_2O$ produced the elimination of 1 equiv of hydrochloric acid and the formation of the binuclear complex **4** in which one cobalt is in an octahedral environment featuring two κ^3-coordinated deprotonated ligands whereas the second cobalt center is detected in tetrahedral coordination geometry, bound to the octahedral cobalt via two phenoxo bridging moieties. Interestingly *L2*-H, (3-^{t}Bu-2-phenol)*bis*(3,5-Me$_2$-pyrazol-1-yl)methane (*L4*-H), or (5-^{t}Bu-2-phenol)*bis*(3,5-Me$_2$-pyrazol-1-yl)methane (*L5*-H) were not oxidized in the reaction with $CuCl_2$. The reaction of the ligand *L2*-H with $ZnCl_2$ and $CuCl_2 \cdot 2H_2O$ yielded the κ^2-coordinated tetrahedral complex **5** and the square planar complex **6**, respectively. The application of the cobalt complex **1** as molecular dosimeter for H_2S was explored and compared to that of the zinc analogue **2**. Density functional theory (DFT) calculations and NMR experiments to assess the possible mechanisms of H_2S detection by both **1** and **2** are also described.

Introduction

Heteroscorpionate ligands have been widely investigated for their application in coordination, organometallic, and bioinorganic chemistry. These ligands are derivatives of poly(pyrazolyl)borates, or *scorpionates*, ligands in which one of the three pyrazole groups is replaced with a different substituted pyrazolyl group or with a coordinating tethered group, containing a coordinating donor, for example, -SR, -NR_2, -Ar. The term *heteroscorpionate* also applies to tridentate ligands in which a main group element, for example, Ga, In, Al, C, Si, replaces B. A large variety of tridentate, neutral, or anionic ligands, where the tethered coordinating site or the atom bridging the two pyrazolyl moieties were changed, have been synthesized.[1,2] Typical examples of tridentate heteroscopionates are based on substituted bis(pyrazolyl)-methane, $HC(pz)_2R'$, where the R′ group is, for example, phenol,[3] thiophenol,[4] carboxyl,[5] or dithiocarboxyl group.[6]

In our research group we devoted particular attention to the phenol-substituted bis(pyrazolyl)methane derivatives.[7−14] Recently the coordination of (3,5-^{t}Bu$_2$-2-phenol)bis(3,5-Me$_2$-pyrazol-1-yl)methane ligand (*L1*-H) to the acidic Zn^{2+} center has been described.[7] The complexes exhibit a tetrahedral

*To whom correspondence should be addressed. E-mail: smilione@unisa.it.

(1) Trofimenko, S. *Scorpionates: The coordination Chemistry of Polypyrazolylborate Ligands*; Imperial College Press: London, 1999.
(2) Pettinari, C. *Scorpionates: II chelating borate ligands*; Imperial College Press: London, 2008.
(3) Higgs, T. C.; Carrano, C. J. *Inorg. Chem.* **1997**, *36*, 298–306.
(4) Higgs, T. C.; Ji, D.; Czernuszewicz, R. S.; Matzanke, B. F.; Schunemann, V.; Trautwein, A. X.; Helliwell, M.; Ramirez, W.; Carrano, C. J. *Inorg. Chem.* **1998**, *37*, 2383–2392.
(5) Otero, A.; Fernandez-Baeza, J.; Tejeda, J.; Antinolo, A.; Carrillo-Hermosilla, F.; ez-Barra, E.; Lara-Sanchez, A.; Fernandez-Lopez, M.; Lanfranchi, M.; Pellinghelli, M. A. J. *Chem. Soc.,-Dalton Trans.* **1999**, 3537–39.
(6) Otero, A.; Fernandez-Baeza, J.; Antinolo, A.; Carrillo-Hermosilla, F.; Tejeda, J.; Lara-Sanchez, A.; Sanchez-Barba, L.; Fernandez-Lopez, M.; Rodriguez, A. M.; Lopez-Solera, I. *Inorg. Chem.* **2002**, *41*, 5193–5202.
(7) Milione, S.; Capacchione, C.; Cuomo, C.; Strianese, M.; Bertolasi, V.; Grassi, A. *Inorg. Chem.* **2009**, *48*, 9510–9518.
(8) Cuomo, C.; Milione, S.; Grassi, A. *Macromol. Rapid Commun.* **2006**, *27*, 611–618.

 Published on Web 01/07/2011

geometry in which the ligand is N,N-κ^2-coordinated to the metal and the hydroxyl phenyl group is not coordinated but is involved in extended intermolecular hydrogen bonding. An unexpected exchange reaction promoted by bis-pyrazolylmethane was observed revealing the influence of the noncoordinating active sites on the stability/reactivity of these complexes.[7]

In this study we extended our investigation to the middle and late transition metals, cobalt and copper. These metals have been widely used to obtain metal-substituted proteins as spectroscopic surrogates of Zn(II) analogues.[15] Comparisons of Zn, Co, and Cu complexes featuring biologically relevant "N_2O" coordination sphere are of great interest. The relative ability of surrogate metal ions to act as functional replacements is still obscure as in the case of metal-substituted enzymes in which the activity can be retained or lost at variance with the metal center. As explanatory example the substitution of Cu(II) or Co(II) for Zn in the metalloproteases astacin and serralysin gives active enzymes whereas that with Ni(II) or Hg(II) does not.[16]

The coordination ability of bis(pyrazol-1-yl)-2-phenylmethane ligands to Co(II), Cu(II), and Zn(II) ions has already been explored to some extent.[17−19] In these studies the heteroscorpionate ligands were mainly employed as anionic ligands to coordinate the metal center through two pyrazole nitrogens and the oxygen of the phenolate group, resulting in a facial coordination of the mixed-donor set. In most of these complexes, Zn(II) is reliably tetrahedral while Co(II) and Cu(II) show a much stronger tendency to expand their coordination sphere and to adopt an octahedral geometry. Mononuclear "sandwich" complexes or homometallic di- and trinuclear species were obtained depending on the degree of substitution on the pyrazole arms and on the experimental conditions.[19] The coordination behavior and the reactivity of the corresponding neutral ligands is not common and easily predictable: the OH phenyl group could be either involved or not in the coordination to the metal center. Furthermore, it could undergo chemical modifications (e.g., deprotonation or redox reactions). We also aimed at shedding light on the possible role of the substituents on the reactivity of the pendant phenol group. For these reasons three differently phenol substituted bis-pyrazolyl-methane ligands (2-phenol-bis(3,5-Me_2-pyrazol-1-yl)methane (*L2*-H), (3-^{t}Bu-2-phenol)*bis*(3,5-Me_2-pyrazol-1-yl)methane (*L4*-H), and (5-^{t}Bu-2-phenol)*bis*(3,5-Me_2-pyrazol-1-yl)methane (*L5*-H)) were included in this work.

In this paper we also explored, as test case, the potential of the cobalt (*L1*-H)$CoCl_2$ (**1**) and zinc (*L1*-H)$ZnCl_2$ (**2**) complexes as H_2S molecular recognition elements. According to the HSAB (Hard and Soft Acids and Bases) theory, both cobalt and zinc ions are "borderline" soft Lewis acids[20] and therefore good candidates for binding soft Lewis bases like H_2S.

Experimental Section

Reagents and Materials. All syntheses were carried out using reaction grade chemicals as received, unless otherwise noted. (3,5-^{t}Bu$_2$-2-phenol)*bis*(3,5-Me_2-pyrazol-1-yl)methane (*L1*-H),[21] 2-phenol-bis(3,5-Me_2-pyrazol-1-yl)methane[17] (*L2*-H), and (*L1*-H)-$ZnCl_2$[7] (**2**) were prepared as previously reported. Elemental analyses were performed with a PERKIN-Elmer 240-C. Mass spectrometry analyses were carried out using a Micromass Quattro micro API triple quadrupole mass spectrometer equipped with an electrospray ion source (Waters, Milford, MA). Room temperature ^{1}H NMR spectra were recorded on a Bruker AVANCE 400 NMR instrument. All spectra were recorded in 5 mm o.d. NMR tubes. The chemical shifts were reported in δ (ppm) referenced to $SiMe_4$ using the residual proton impurities of the deuterated solvent. Typically, 6 mg of the complexes in 0.6 mL of CD_2Cl_2 were used for each experiment. An inversion−recovery pulse sequence was used to measure longitudinal relaxation times. The T_1 values were obtained from a two-parameter fit of the data to an exponential recovery function.

Synthesis of (3-^{t}Bu-2-phenol)*bis*(3,5-Me_2-pyrazol-1-yl)methane (*L4*-H). Bis(3,5-Me_2-pyrazol-1-yl)ketone[17] (1.00 g, 4.58 mmol), 3-^{t}Bu-salicylaldehyde (0.82 g, 4.58 mmol), and $CoCl_2\cdot 6H_20$ (0.02 g, 0.08 mmol) were placed in a 100 cm^3 round-bottomed flask. The mixture was then heated to 120 °C. During this time the mixture turned to dark blue and evolution of CO_2 was observed. The mixture was cooled to RT, CH_2Cl_2 (40 cm^3) was added, and the flask shaken until a pink solution formed. This solution was extracted two times with H_2O (2 × 40 cm^3), separated and dried over $MgSO_4$ for 16 h. Hexane (60 cm^3) was then added and CH_2Cl_2 was removed by rotary evaporation, causing the precipitation of a pale beige solid which was collected by filtration, washed with hexane (20 cm^3), and dried in vacuo. Yield: 0.79 g, 49%. Anal. Calcd for *L4*-H $C_{21}H_{28}N_4O$: C, 71.56; H, 8.01; N, 15.90. Found: C, 72.03; H, 8.56; N, 15.84. ^{1}H NMR (400 MHz, $CDCl_3$, 20 °C): δ 1.41 (s, 9H, 3-tBu-Ph), 2.09 (s, 6H, 5-CH_3-Pz), 2.19 (s, 6H, 3-CH_3-Pz), 5.85 (s, 2H, Pz-H), 6.79 (m, 2H, 5-Ph + 6-Ph), 7.30 (s, 1H, −CH−), 7.32 (dd, 1H, J = 7.1 Hz, J = 2.4 Hz 4-Ph). MS (ESI acetonitrile): m/z (%) 728.02 (70) [(*L4*-H)$_2$]Na$^+$, 375.67 (35) [(*L4*-H)]Na$^+$.

Synthesis of (5-^{t}Bu-2-phenol)*bis*(3,5-Me_2-pyrazol-1-yl)methane (*L5*-H). The procedure was the same used for **L4-H**. The reagents and reactant ratios were bis(3,5-Me_2-pyrazol-1-yl)ketone (1.00 g, 4.58 mmol), 5-^{t}Bu-salicylaldehyde (0.82 g, 4.58 mmol), and $CoCl_2\cdot 6H_20$ (0.02 g, 0.08 g mmol). Yield: 0.87 g, 53%. Anal. Calcd for *L5*-H $C_{21}H_{28}N_4O$: C, 71.56 H, 8.01; N, 15.90. Found: C, 72.06; H, 8.39; N, 15.79. ^{1}H NMR (400 MHz, $CDCl_3$, 20 °C): δ 1.24 (s, 9H, 5-tBu-Ph), 2.14 (s, 6H, 5-CH_3-Pz), 2.18 (s, 6H, 3-CH_3-Pz), 5.83 (s, 2H, Pz-H), 6.91 (d, 1H, J = 8.6 Hz, 3-Ph), 6.98 (d, 1H, J = 2.2 Hz, 6-Ph), 7.20 (s, 1H, −CH−), 7.27 (dd, 1H, J = 8.8 Hz, J = 2.2 Hz, 4-Ph). MS (ESI acetonitrile): m/z (%) 762.96 (100) [(*L5*-H)$_2$-(H_2O)]K$^+$, 375.74 (10) [(*L5*-H)]Na$^+$.

Synthesis of (*L1*-H)$CoCl_2$ (1). A solution of *L1*-H (200 mg, 0.489 mmol) in tetrahydrofuran (THF, 1.5 mL) was added to a solution of $CoCl_2\cdot 6H_2O$ (116 mg, 0.489 mmol) in THF (1.5 mL). The mixture was stirred for 1 h at room temperature (RT). A bright blue crystalline solid was isolated after cooling

(9) Milione, S.; Montefusco, C.; Cuenca, T.; Grassi, A. *Chem. Commun.* **2003**, 1176–1177.
(10) Milione, S.; Bertolasi, V.; Cuenca, T.; Grassi, A. *Organometallics* **2005**, *24*, 4915–4925.
(11) Milione, S.; Grisi, F.; Centore, R.; Tuzi, A. *Organometallics* **2006**, *25*, 266–274.
(12) Milione, S.; Cuomo, C.; Grassi, A. *Top. Catal.* **2006**, *40*, 163–172.
(13) Paolucci, G.; Bortoluzzi, M.; Milione, S.; Grassi, A. *Inorg. Chim. Acta* **2009**, *362*, 4353–4357.
(14) Silvestri, A.; Grisi, F.; Milione, S. *J. Polym. Sci., Polym. Chem.* **2010**, *48*, 3632–3639.
(15) Salgado, J.; Kalverda, A. P.; Diederix, R. E. M.; Canters, G. W.; Moratal, J. M.; Lawler, A. T.; Dennison, C. *J. Biol. Inorg. Chem.* **1999**, *4*, 457–467.
(16) Auld, D. S. *Proteolytic Enzymes: Aspartic and Metallo Peptidases*; Barrett, A. J., Ed.; Academic Press: San Diego, CA, 1995; Vol. *248*, pp 228−242.
(17) Higgs, T. C.; Dean, N. S.; Carrano, C. J. *Inorg. Chem.* **1998**, *37*, 1473–1482.
(18) Higgs, T. C.; Spartalian, K.; O'Connor, C. J.; Matzanke, B. F.; Carrano, C. J. *Inorg. Chem.* **1998**, *37*, 2263–2272.
(19) Higgs, T. C.; Carrano, C. J. *Inorg. Chem.* **1997**, *36*, 291–297.
(20) Pearson, R. G. *J. Am. Chem. Soc.* **1963**, *85*, 3533–3539.
(21) Hammes, B. S.; Carrano, C. J. *Inorg. Chem.* **1999**, *38*, 3562–3568.

the filtrate solution down to −20 °C. Yield: 145 mg (55%). X-ray crystals were grown from a THF/CH_2Cl_2 solution at −20 °C.

Anal. Calcd for **1**·THF·CH_2Cl_2 $C_{30}H_{46}N_4O_2CoCl_4$: C, 51.81; H, 6.68; N, 8.06. Found: C, 51.20; H, 6.48; N, 8.54. ^{1}H NMR (400 MHz, CD_2Cl_2, 20 °C): δ −18.97 (s, 6H, 3-CH_3-Pz), 0.12 (s, 9H, 5-tBu-Ph), 2.64 (s, 9H, 3-tBu-Ph), 9.57 (s, 1H, 4-Ph), 9.88 (s, 1H, −OH), 21.09 (s, 1H, −CH−), 38.85 (s, 2H, Pz-H), 42.93 (s, 6H, 5-CH_3-Pz). MS (ESI acetonitrile): *m*/*z* (%) 507.49 (100) [(*L1*-H)Co(H_2O)]Na^+, 562.52 (15) [(*L1*-H)Co(H_2O)$_4$]Na^+.

Synthesis of (*L3*)$CuCl_2$ (3) (*L3* = 2-^{t}Bu-6-(bis(3,5-Me_2-pyrazol-1-yl)methyl)cyclohexa-2,5-diene-1,4-dione). A solution of *L1*-H (200 mg, 0.489 mmol) in THF (1.0 mL) was slowly added to a solution of $CuCl_2·6H_2O$ (83 mg, 0.489 mmol) in THF (1.0 mL). The mixture was stirred for 5 h at RT. Pale yellow crystals were isolated after cooling the filtrate solution down to −20 °C. Yield: 150 mg (61%). X-ray crystals were grown by slow diffusion of Et_2O in a CH_3CN solution of **3**. Anal. Calcd for **3** $C_{21}H_{26}N_4O_2CuCl_2$: C, 50.35; H, 5.24; N, 11.19. Found: C, 50.68; H, 5.12; N, 10.98. MS (ESI acetonitrile): *m*/*z* (%) 469.86 (100) [(*L3*)Cu(H_2O)]Na^+, 388.91 (30) [(*L3*)]Na^+.

Synthesis of (*L2*)$_2Co_2Cl_2$ (4). A suspension of *L2*-H (200 mg, 0.675 mmol) in THF (5.5 mL) was added to a solution of $CoCl_2·6H_2O$ (160 mg, 0.675 mmol) in THF (1.5 mL). The mixture was stirred overnight at RT. A bright blue crystalline solid was isolated. Yield: 200 mg (40%). X-ray crystals were grown from CH_2Cl_2 solution at −20 °C. Anal. Calcd for **4**·CH_2Cl_2 $C_{35}H_{40}Cl_4Co_2N_8O_2$: C, 48.63; H, 4.67; N, 12.97. Found: C, 48.52; H, 4.73; N, 12.85. MS (ESI acetonitrile): *m*/*z* (%) 650.74 (100) [(*L2*-*H*)(*L2*)Co]$^+$.

Synthesis of (*L2*-H)$ZnCl_2$ (5). A solution of *L2*-H (100 mg, 0.340 mmol) in CH_2Cl_2 (5 mL) was added to a solution of $ZnCl_2$ (45 mg, 0.340 mmol) in THF (0.5 mL). The mixture was stirred for 1 h at RT. A colorless crystalline solid was isolated after cooling the filtrate solution down to −20 °C. Yield: 90 mg (60%). X-ray crystals were grown from a THF/CH_2Cl_2 solution at −20 °C. Anal. Calcd for **5** $C_{17}H_{20}Cl_2N_4OZn$: C, 47.19; H, 4.67; N, 12.95. Found: C, 47.11; H, 4.61; N, 12.80. ^{1}H NMR (400 MHz, CD_2Cl_2, 20 °C): ^{1}H NMR (400 MHz, CD_2Cl_2, 20 °C): δ 2.48 (s, 6H, 5-CH_3-Pz), 2.50 (s, 6H, 3-CH_3-Pz), 6.11 (s, 2H, Pz-H), 6.73 (d, 1H, *J* = 8.2 Hz, 3-Ph), 6.92 (t, 1H, *J* = 8.4 Hz, 4-Ph) 7.13 (d, 1H, *J* = 7.5 Hz, 6-Ph), 7.22 (t, 1H, *J* = 7.3 Hz, 5-Ph), 7.62 (s, 1H, −CH−). MS (ESI acetonitrile): *m*/*z* (%) 395.64 (100) [(*L2*-*H*)ZnCl]$^+$.

Synthesis of (*L2*-H)$CuCl_2·H_2O$ (6). A solution of *L2*-H (50 mg, 0.177 mmol) in CH_2Cl_2 (2.5 mL) was added to a solution of $CuCl_2·2H_2O$ (30 mg, 0.177 mmol) in THF (0.5 mL). The mixture was stirred for 1 h at RT. A bright green crystalline solid was isolated after cooling the filtrate solution down to −20 °C. Yield: 30 mg (40%). X-ray crystals were grown from a THF/CH_2Cl_2 solution at −20 °C. Anal. Calcd for. **6**·2(H_2O) $C_{17}H_{26}Cl_2CuN_4O_4$: C, 42.11; H, 5.41; N, 11.56. Found: C, 42.03; H, 5.48; N, 12.04. MS (ESI acetonitrile): *m*/*z* (%) 654.65 (100) [(*L2*-H)(*L2*)Cu], 400.46 (35) [(*L2*-H)Cu(H_2O)]Na^+.

Synthesis of (*L1*-H)$CuCl_2$ (7). In drybox, a solution of *L1*-H (300 mg, 0.734 mmol) in anhydrous and deareated THF (2.0 mL) was slowly added to a solution of $CuCl_2·2H_2O$ (125 mg, 0.734 mmol) in degassed THF (1.0 mL). The mixture was stirred for 5 h at RT. A pale green powder was isolated after cooling the filtrate solution down to −20 °C. Yield: 225 mg (56%). Anal. Calcd for **7** $C_{25}H_{36}N_4OCuCl_2$: C, 55.29; H, 6.68; N, 10.32. Found: C, 56.16; H, 7.01; N, 9.87. MS (ESI acetonitrile): *m*/*z* (%) 512.70 (20) [(*L1*)Cu(H_2O)]Na^+.

Synthesis of (*L4*-H)$CuCl_2$ (8). A solution of *L4*-H (100 mg, 0.283 mmol) in CH_2Cl_2 (0.8 mL) was slowly added to a solution of $CuCl_2·2H_2O$ (48 mg, 0.283 mmol) in THF (0.5 mL). The mixture was stirred for 5 h at RT. A pale green powder was isolated after cooling the filtrate solution down to −20 °C. Yield: 75 mg (55%). Anal. Calcd for **8** $C_{21}H_{28}N_4OCuCl_2$: C, 51.80; H, 5.80; N, 11.51. Found: C, 53.01; H, 6.20; N, 10.97. MS (ESI acetonitrile): *m*/*z* (%) 449.49 (40) [(*L4*-H)CuCl]$^+$, 490.61 (75) [(*L4*)CuCl(H_2O)]Na^+.

Synthesis of (*L5*-H)$CuCl_2$ (9). The same procedure as for (*L4*-H)$CuCl_2$ (**8**) (vide supra) was used with the following amounts of reagents: *L5*-H (100 mg, 0.283 mmol), $CuCl_2·2H_2O$ (48 mg, 0.283 mmol), THF (0.5 mL). Yield: 90 mg (66%). Anal. Calcd for **9** $C_{21}H_{28}N_4OCuCl_2$: C, 51.80; H, 5.80; N, 11.51. Found: C, 53.06; H, 6.14; N, 10.83. MS (ESI acetonitrile): *m*/*z* (%) 449.55 (30) [(*L5*-H)CuCl]$^+$, 490.57 (70) [(*L5*)CuCl(H_2O)]Na^+.

H_2S-Saturated Solutions. Saturated dichloromethane solutions of H_2S were prepared by bubbling H_2S gas through 5 mL of CH_2Cl_2 for 1 h resulting in an approximate concentration of 0.53 M at 20 °C.[22] H_2S gas was produced in situ according to literature procedures.[23]

Absorbance and Fluorescence Measurements. Absorption spectra were recorded on a Cary-50 Spectrophotometer, using a 1 cm quartz cuvette (Hellma Benelux bv, Rijswijk, Netherlands) and a slit-width equivalent to a bandwidth of 5 nm. Binding constants for 1:1 complexation were obtained by a nonlinear least-squares fit[24] of the absorbance (*A*) versus the concentration of the ligand *L1*-H added, according to the following equation:

$$A = A_0 + [(A_{lim} - A_0)/2c_0][c_0 + c_L + 1/K_a - [(c_0 + c_L + 1/K_a)^2 - 4c_0c_L]^{1/2}]$$

where A_0 and A are the absorbances of the complex at a selected wavelength in the absence and presence of the ligand *L1*-H, respectively; c_0 is the total concentration of the Co^{2+} ion; c_L is the concentration of *L1*-H; A_{lim} is the limiting value of the absorbance in the presence of a large excess of *L1*-H, and K_a is the stability constant.

Fluorescence spectra were measured on a Cary Eclipse Spectrophotometer in a 10 × 10 mm^2 airtight quartz fluorescence cuvette (Hellma Benelux bv, Rijswijk, Netherlands) with an emission band-pass of 10 nm and an excitation band-pass of 5 nm. Both absorption and fluorescence measurements were performed in dichloromethane solutions at RT. The H_2S titration experiments were performed as follows: the cuvette was filled with sample solutions in dichloromethane. Then microliter amounts of H_2S-saturated dichloromethane solutions (to the end concentrations specified in the figure captions) were injected via a gastight syringe at intervals of 1 min between subsequent additions. The experiment ended when no changes in the fluorescence intensities could be detected upon H_2S addition.

^{1}H NMR H_2S titrations for **1** and **2** were performed at 25 °C in CD_2Cl_2. A total of 6 spectra were registered varying the H_2S concentration in the range of 0.150−0.350 M. The complex concentration was 0.010 M.

Crystal Structure Determinations. The crystal data of compounds (*L1*-H)$CoCl_2$ (**1**), (*L3*)$CuCl_2$ (**3**), (*L2*)$_2Co_2Cl_2$ (**4**), (*L2*-H)$ZnCl_2$ (**5**), and (*L2*-H)$CuCl_2$ (**6**) were collected at RT using a Nonius Kappa CCD diffractometer with graphite monochromated Mo−Kα radiation. The data sets were integrated with the Denzo-SMN package[25] and corrected for Lorentz, polarization and absorption effects.[26] The structures were solved by direct methods[27] and refined using full-matrix least-squares with all

(22) Barnabas, F. A.; Sallin, D.; James, B. R. *Can. J. Chem.* **1989**, *67*, 2009–2015.
(23) Mattson B.; Anderson M.; Mattson S. *Microscale Gas Chemistry*, (book) 4th ed.; Educational Innovations: Norwalk, CT, 2003.
(24) Bourson, J.; Pouget, J.; Valeur, B. *J. Phys. Chem.* **1993**, *97*, 4552–57.
(25) Otwinowski, Z.; Minor, W. Processing of X-ray Diffraction Data Collected in Oscillation Mode. In *Methods in Enzymology: Macromolecular Crystallography*, part A; Academic Press: San Diego, CA, 1997; pp 307−326.
(26) Blessing, R. H. *Acta Crystallogr., Sect. A* **1995**, *51*(Pt 1), 33–38.
(27) Altomare, A.; Burla, M. C.; Camalli, M.; Cascarano, G. L.; Giacovazzo, C.; Guagliardi, A.; Moliterni, A. G. G.; Polidori, G.; Spagna, R. *J. Appl. Crystallogr.* **1999**, *32*, 115–19.

Table 1. Crystallographic Data

compound	(*L1*-H)$CoCl_2$ (**1**)	(*L3*)$CuCl_2$ (**3**)	$(L2)_2Co_2Cl_2$ (**4**)	(*L2*-H)$ZnCl_2$ (**5**)	(*L2*-H)$CuCl_2 \cdot H_2O$ (**6**)
formula	$C_{25}H_{36}Cl_2CoN_4O \cdot CH_2Cl_2 \cdot C_4H_8O$	$C_{21}H_{26}Cl_2CuN_4O_2$	$C_{34}H_{38}Cl_2Co_2N_8O_2 \cdot CH_2Cl_2$	$C_{17}H_{20}Cl_2N_4OZn$	$C_{17}H_{22}Cl_2CuN_4O_2 \cdot 2(H_2O)$
M	695.44	500.90	864.41	432.64	484.86
space group	$P2_1/c$	Cc	$R\bar{3}c$	Cc	$P2_1/n$
crystal system	monoclinic	monoclinic	trigonal	monoclinic	monoclinic
a/Å	9.0399(4)	9.4281(3)	19.6685(3)	9.1544(8)	8.6189(2)
b/Å	20.0369(8)	18.9355(7)	19.6685(3)	14.4953(13)	14.6164(5)
c/Å	19.6152(9)	13.3689(5)	53.1546(6)	15.0072(14)	16.9787(6)
α/deg	90	90	90	90	90
β/deg	92.463(2)	91.056(2)	90	103.606(4)	101.775(1)
γ/deg	90	90	120	90	90
U/Å^3	3549.6(3)	2386.3(2)	17807.9(4)	1935.5(3)	2093.9(1)
Z	4	4	18	4	4
T/K	295	295	295	295	295
D_c/g cm^{-3}	1.301	1.394	1.451	1.485	1.538
F(000)	1460	1036	7992	888	1004
μ(Mo−Kα)/cm^{-1}	8.16	11.63	11.50	15.57	15.38
measured reflections	10325	11593	21049	5614	13583
unique reflections	6050	2821	4317	2988	4813
R_{int}	0.0463	0.0318	0.0357	0.0870	0.0320
obs. reflns [$I \geq 2\sigma(I)$]	3528	2433	3291	2401	3668
$\theta_{min}-\theta_{max}$/deg	2.72−25.00	5.21−28.00	2.37−27.00	5.59−25.32	3.37−27.55
hkl ranges	−10,10;−23,21;−23,23	−12,12;−21,24;−17,17	−25,19;−21,21;−67,67	−10,10;−17,17;−17,17	−11,11;−16,19;−22,22
$R(F^2)$ (obs.reflns)	0.0734	0.0365	0.0530	0.0636	0.0385
$wR(F^2)$ (all reflns)	0.2279	0.0948	0.1637	0.1717	0.1018
no. variables	364	278	236	230	269
goodness of fit	1.024	1.053	1.057	1.024	1.035
$\Delta\rho_{max}$; $\Delta\rho_{min}$ /e Å^{-3}	0.58; −0.45	0.41;−0.35	1.18;−0.92	0.66;−0.43	0.33;−0.50

non-hydrogen atoms anisotropically and hydrogens included on calculated positions, riding on their carrier atoms. (*L1*-H)$CoCl_2$ (**1**) contains two solvent molecules, CH_2Cl_2 and THF, which display some disorder. Furthermore, the methyl groups in a *t*Butyl group were found disordered and refined isotropically over two positions with occupation factors of 0.50 each. The asymmetric unit of $(L2)_2Co_2Cl_2$ (**4**) contains one-half of the dimetallic molecule, both Co1 and Co2 atoms being located on a 2-fold C_2 rotation axis, and one-half of the solvent molecule CH_2Cl_2 located on a 2-fold axis passing through the Carbon atom. The asymmetric unit of (*L2*-H)$CuCl_2$ (**6**) contains the square pyramidal complex of Cu(II) with a water molecule coordinated in apical position and two other non-coordinated water molecules.

All calculations were performed using SHELXL-97[28] and PARST[29] implemented in the WINGX[30] system of programs. The crystal data are given in Table 1. Selected bond distances and angles are given in Tables 2, 3, and 4.

Crystallographic data (excluding structure factors) have been deposited at the Cambridge Crystallographic Data Centre and allocated the deposition numbers CCDC 773833: (*L1*-H)$CoCl_2$ (**1**); 777333: (*L3*)$CuCl_2$ (**3**); 784827: $(L2)_2Co_2Cl_2$ (**4**); 784828: (*L2*-H)$ZnCl_2$ (**5**); 784829: (*L2*-H)$CuCl_2$(**6**). These data can be obtained free of charge via www.ccdc.cam.ac.uk/conts/retrieving.html or on application to CCDC, Union Road, Cambridge, CB2 1EZ, U.K. [fax: (+44)1223−336033, e-mail: deposit@ccdc.cam.ac.uk]

Results and Discussion

Direct treatment of (3,5-^{t}Bu$_2$-2-phenol)bis(3,5-Me$_2$-pyrazol-1-yl)methane (*L1*-H) with 1 equiv of $CoCl_2 \cdot 6H_2O$ at RT afforded the mononuclear tetrahedral complex (*L1*-H)$CoCl_2$ (**1**) in good yield (Scheme 1). Single crystal of **1** suitable for X-ray diffraction were grown from a THF/CH_2Cl_2 solution at −20 °C (Table 1); the ORTEP[31] view of complex **1** is shown in Figure 1. The cobalt(II) metal center is tetrahedrally κ^2-N, N coordinated by two pyrazole rings of *L1*-H and two chloride ligands. The dihedral angle between the Cl1−Co−Cl2 and N1−Co−N2 planes is of 89.5(1)°, a value very close to the ideal one of 90°. The slight distortion from the ideal tetrahedral coordination is mainly determined by the N−Co−N angle of 93.4(2)° constrained by the bite of bischelating ligand. The Co−Cl distances of 2.227(2) and

Table 2. Selected Geometrical Parameters (Å and degrees) for Compounds (**1**) and (**3**)[a]

(*L1*-H)$CoCl_2$ (**1**)		(*L3*)$CuCl_2$ (**3**)	
Distances			
Co1−Cl1	2.227(2)	Cu1−Cl1	2.217(1)
Co1−Cl2	2.231(2)	Cu1−Cl2	2.188(2)
Co1−N1	2.019(5)	Cu1−N2	2.091(4)
Co1−N3	2.028(4)	Co1−N4	1.975(4)
Angles			
Cl1−Co1−Cl2	111.2(1)	Cl1−Cu1−Cl2	101.2(1)
Cl1−Co1−N1	116.0(1)	Cl1−Cu1−N2	136.2(1)
Cl1−Co1−N3	116.2(1)	Cl1−Cu1−N4	96.6(1)
Cl2−Co1−N1	109.9(1)	Cl2−Cu1−N2	104.8(1)
Cl2−Co1−N3	108.9(1)	Cl2−Cu1−N4	137.5(1)
N1−Co1−N3	93.4(2)	N2−Cu1−N4	87.4(2)
Torsion Angles			
C1−C6−C7−N2	75.3(6)	C1−C6−C7−N1	170.7(4)
C1−C6−C7−N4	−157.9(5)	C1−C6−C7−N3	47.9(5)
Dihedral Angles			
Cl1−Co1−Cl2 ^ N1−Co1−N3	89.5(1)	Cl1−Cu1−Cl2 ^ N2−Cu1−N4	59.1(1)
N1−N2−C8−C9−C10 ^ N3−N4−C13−C14−C15	138.6(2)	N1−N2−C8−C9−C10 ^ N3−N4−C13−C14−C15	130.0(2)

[a] (^) stands for dihedral angle.

(28) Sheldrich, G. M. *SHELXTL-97, Program for the Solution of Crystal Structure Refinement*; University of Göttingen: Göttingen, Germany, 1997.
(29) Nardelli, M. *J. Appl. Crystallogr.* **1995**, *28*, 659.
(30) Farrugia, L. J. *J. Appl. Crystallogr.* **1999**, *32*, 837–838.

Table 3. Selected Geometrical Parameters (Å and degrees) for Compound (**4**)[a]

$(L2)_2Co_2Cl_2$ (**4**)			
Distances			
Co1−O1	2.094(3)	Co2−Cl1	2.224(1)
Co1−N2	2.157(3)	Co2−O1	1.981(2)
Co1−N4	2.127(3)		
Angles			
O1−Co1−N2	85.7(1)	O1−Co2−Cl1	111.2(1)
O1−Co1−N4	92.1(1)	O1−Co2−Cl1′	116.6(1)
O1−Co1−N4′	168.5(1)	O1−Co2−O1′	82.2(1)
O1−Co1−O1′	76.9(1)	Cl1−Co2−Cl1′	115.0(1)
N2−Co1−N4	83.7(1)	Co1−O1−Co2	100.4(1)
N2−Co1−N2′	176.8(1)		
N4−Co1−N4′	99.0(1)		
Torsion Angles			
C1−C6−C7−N1	47.5(5)	C1−C6−C7−N3	−80.9(4)
Dihedral Angles			
Cl1−Co2−Cl1′ ^ O1−Co2−O1′	90	N1−N2−C8−C9−C10^ N3−N4−C13−C14−C15	121.9(2)

[a] (^) stands for dihedral angle.

Table 4. Selected Geometrical Parameters (Å and degrees) for Compounds (**5**) and (**6**)[a]

$(L2$-H$)ZnCl_2$ (**5**)		$(L2$-H$)CuCl_2\cdot H_2O$ (**6**)	
Distances			
Zn1−Cl1	2.194(3)	Cu1−Cl1	2.291(1)
Zn1−Cl2	2.269(3)	Cu1−Cl2	2.316(1)
Zn1−N2	2.028(8)	Cu1−N2	2.037(2)
Zn1−N4	2.026(9)	Cu1−N4	2.039(2)
		Cu1−O1w	2.244(2)
Angles			
Cl1−Zn1−Cl2	113.9(1)	Cl1−Cu1−Cl2	89.82(3)
Cl1−Zn1−N2	119.8(2)	Cl1−Cu1−N2	91.55(6)
Cl1−Zn1−N4	115.6(2)	Cl1−Cu1−N4	170.88(6)
Cl2−Zn1−N2	106.0(2)	Cl2−Cu1−N2	164.96(7)
Cl2−Zn1−N4	105.5(2)	Cl2−Cu1−N4	90.65(5)
N2−Zn1−N4	93.4(3)	N2−Cu1−N4	85.67(8)
		Cl1−Cu1−O1w	94.03(7)
		Cl2−Cu1−O1w	95.45(7)
		N2−Cu1−O1w	99.39(9)
		N4−Cu1−O1w	94.99(9)
Torsion Angles			
C1−C6−C7−N1	−59.1(11)	C1−C6−C7−N1	−57.2(3)
C1−C6−C7−N3	174.2(8)	C1−C6−C7−N3	179.6(2)
Dihedral Angles			
Cl1−Zn1−Cl2 ^ N1−Zn1−N3	90.9(2)	Cl1−Cu1−Cl2 ^ N2−Cu1−N4	162.93(5)
N1−N2−C8−C9−C10^ N3−N4−C13−C14−C15	136.4(4)	N1−N2−C8−C9−C10^ N3−N4−C13−C14−C15	114.20(8)

[a] (^) stands for dihedral angle.

2.231(2) Å and Co−N (pyrazole) ones of 2.019(5) and 2.028(4) Å are in agreement with the values found in similar complexes.[19,32,33] The geometrical parameters are very similar to those observed in the zinc complex of the same heteroscorpionate ligand (*L1*-H)$ZnCl_2$ (**2**).[7]

Scheme 1

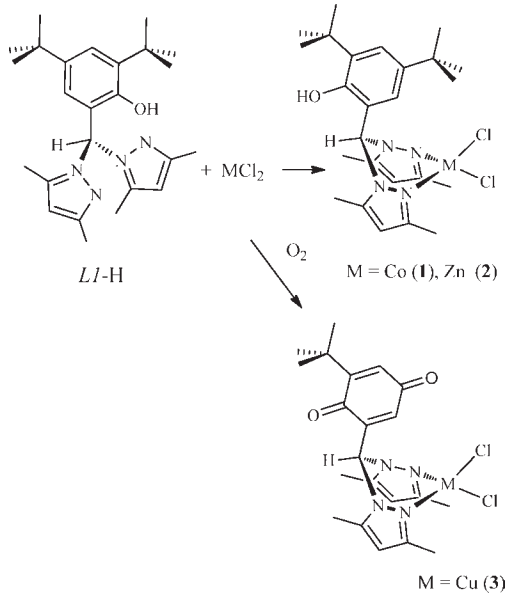

To our surprise, the treatment of *L1*-H with 1 equiv of $CuCl_2\cdot 2H_2O$ afforded the complex (*L3*)$CuCl_2$ (**3**) (*L3* = 2-^{t}Bu-6-(bis(3,5-Me_2-pyrazol-1-yl)methyl)cyclohexa-2,5-diene-1,4-dione). In this reaction the phenol moiety was transformed into the corresponding *para*-benzoquinone residue (Scheme 1, results of an investigation into this reaction are presented in a subsequent paragraph). The heteroscorpionate ligand *L3* is κ^2-coordinated to the tetrahedral metal center through the imino nitrogen atoms of the two pyrazolyl rings. The ORTEP view of the complex **3** is shown in Figure 2. The geometry of the copper atom resembles a tetrahedral arrangement; however, the plane defined by Cu1, Cl1, and Cl2 atoms makes an angle of 121.9(2)° with the plane defined by Cu1, N2, and N4 atoms. Hence, the geometry at the copper is intermediate between square planar and tetrahedral and is better described as distorted tetrahedral because the twist angle is much closer to the 90° angle expected for a tetrahedron as compared to the 180° angle for the square planar description. Distortion from planarity is unusual for Cu(II) complexes, but more common for complexes with large steric hindrance.[34−43] Here, the distorted coordination geometry observed in **3** could be attributed to the steric repulsion between the coordinated Cl and the methyl groups of the pyrazoles. The other structural parameters are in good agreement with those observed in $CuCl_2$ complexes[17] exhibiting distorted pseudotetrahedral geometry.[34−43]

(31) Burnett, M. N.; Johnson, C. K. *ORTEP-III: Oak Ridge Thermal Ellipsoids Plot Program for Crystal Structure Illustration*, ORNL-6895; Oak Ridge National Laboratory: Oak Ridge, TN, 1996.
(32) Santillan, G. A.; Carrano, C. J. *Dalton Trans.* **2008**, 3995–4005.
(33) Li, Q.-Y.; Zhang, W.-H.; Li, H.-X.; Tang, X.-Y.; Lang, J.-P.; Zhang, Y.; Wang, X.-Y.; Gao, S. *Chin. J. Chem.* **2006**, *24*, 1716–1720.
(34) Riggio, I.; van Albada, G. A.; Ellis, D. D.; Mutikainen, I.; Spek, A. L.; Turpeinen, U.; Reedijk, J. *Polyhedron* **2001**, *20*, 2659–2666.
(35) Schuitema, A. M.; Engelen, M.; Koval, I. A.; Gorter, S.; Driessen, W. L.; Reedijk, J. *Inorg. Chim. Acta* **2001**, *324*, 57–64.
(36) Stibrany, R. T.; Schulz, D. N.; Kacker, S.; Patil, A. O.; Baugh, L. S.; Rucker, S. P.; Zushma, S.; Berluche, E.; Sissano, J. A. *Macromolecules* **2003**, *36*, 8584–8586.
(37) Sbai, F.; Regragui, R.; Essassi, E.; Kenz, A.; Pierrot, M. *Acta Crystallogr.; Sect. C* **2003**, *59*, m334–m336.
(38) Shaw, J. L.; Cardon, T. B.; Lorigan, G. A.; Ziegler, C. J. *Eur. J. Inorg. Chem.* **2004**, 1073–1080.
(39) van Albada, G. A.; Mutikainen, I.; Turpeinen, U.; Reedijk, J. *J. Chem. Crystallogr.* **2007**, *37*, 489–496.

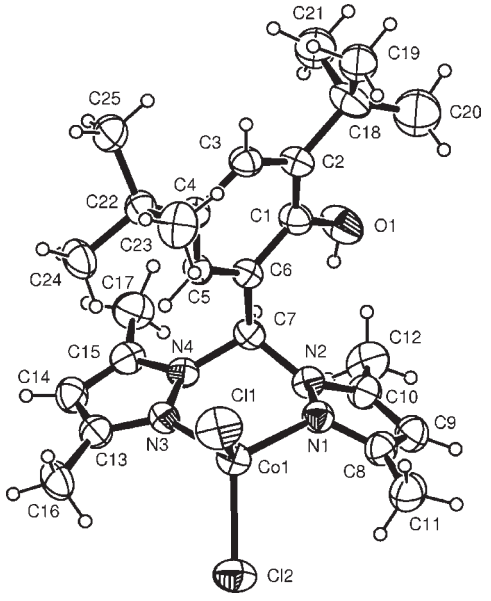

Figure 1. ORTEP view of complex **1** showing the thermal ellipsoids at 30% probability level.

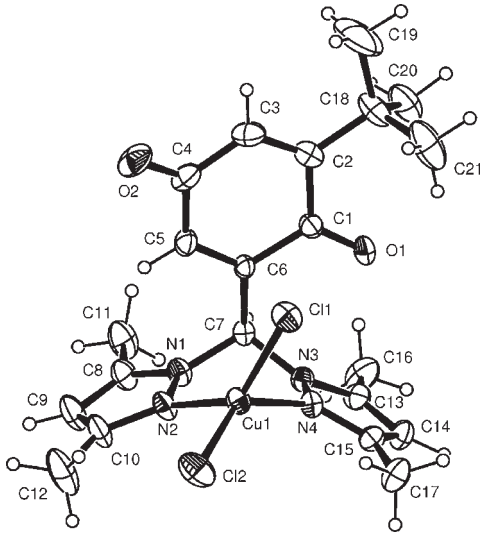

Figure 2. ORTEP view of complex **3** showing the thermal ellipsoids at 30% probability level.

The reaction of $CoCl_2 \cdot 6H_2O$, $ZnCl_2$, and $CuCl_2 \cdot 2H_2O$ with the less sterically hindered *L2*-H ligand led to different products (Scheme 2). Indeed the treatment of *L2*-H with 1 equiv of $CoCl_2 \cdot 6H_2O$ at RT afforded the homometallic dimer $(L2)_2Co_2Cl_2$ (**4**) in which two cobalt atoms exhibit octahedral and tetrahedral coordination environments, respectively. One cobalt atom is coordinated by two tridentate heteroscorpionate ligands through four pyrazole nitrogen atoms and by two phenolate oxygens while the second cobalt atom is coordinated by two chlorine atoms and by the same

Scheme 2

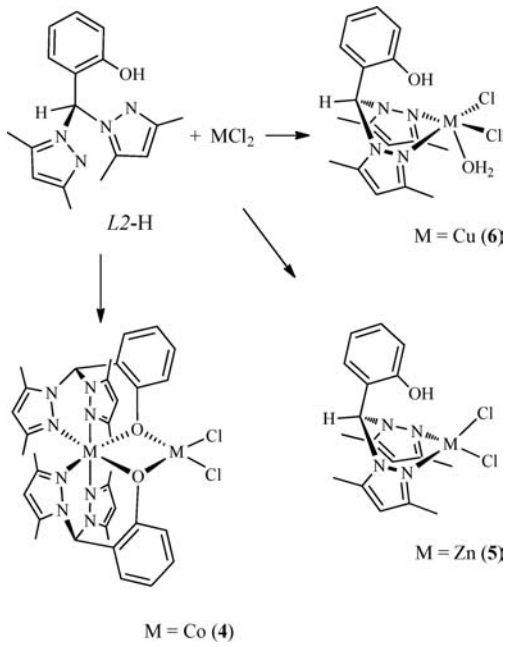

two phenolate oxygens. The ORTEP view of complex **4** is shown in Figure 3. This species had been already obtained by a different synthetic route, that is, by treating the phenolate-*L2* derivative with 1 equiv of $CoCl_2$.[17] Our derivative belongs to a different space group ($R\bar{3}c$ instead of $P2_1/c$) and contains a different solvent molecule (CH_2Cl_2 instead of CH_3CN) per asymmetric unit.

The nuclearity of the cobalt complexes seems to depend on the steric hindrance of the ligand in close proximity to the metal center. Actually, when the methyl groups are replaced by isopropyl groups, as in the case of 2-phenol-bis(3,5-iPr_2-pyrazol-1-yl)methane reported by Higgs and Carrano,[19] the mononuclear tetrahedral complex is obtained.

Interestingly deprotonation of the ligand was not observed in the reaction of *L2*-H with $ZnCl_2$ or $CuCl_2 \cdot 2H_2O$. The mononuclear complexes (*L2*-H)$ZnCl_2$ (**5**) and (*L2*-H)$CuCl_2 \cdot H_2O$ (**6**) bearing the κ^2-coordinated *L2*-H were indeed isolated from the reaction mixture (Scheme 2). Most likely, the less acidic character of the zinc(II) and copper(II) cations hampers the elimination of hydrochloric acid during the reaction under the conditions employed. Interestingly, the oxidation of the phenol group to yield the corresponding *para*-quinone did not occur in the reaction of *L2*-H with $CuCl_2 \cdot 2H_2O$.

The ORTEP view of **5** is shown in Figure 4. The zinc(II) ion displays an almost perfect tetrahedral geometry. The structural parameters are in perfect agreement with those of the analogous complexes. The molecules form, in the crystal, extended chains bound by means of OH(phenolic)$\cdots$Cl hydrogen bonds [O1$\cdots$Cl2 = 3.115 Å].

The ORTEP view of **6** is shown in Figure 5. The copper ion is in a square pyramidal environment with two pyrazole nitrogen atoms and two chlorine atoms on the basal plane and a water molecule in the apical position. This molecule together with other two non-coordinated water molecules and the phenol group form an extended network of hydrogen bonds in the crystals (Supporting Information, Figure S1).

(40) Santillan, G. A.; Carrano, C. J. *Inorg. Chem.* **2007**, *46*, 1751–1759.
(41) Kozlevcar, B.; Pregelj, T.; Pevec, A.; Kitanovski, N.; Costa, J. S.; van Albada, G.; Gamez, P.; Reedijk, J. *Eur. J. Inorg. Chem.* **2008**, 4977–4982.
(42) Drabina, P.; Valenta, P.; Jansa, P.; Ruzicka, A.; Hanusek, J.; Sedlak, M. *Polyhedron* **2008**, *27*, 268–274.
(43) Fujisawa, K.; Kanda, R.; Miyashita, Y.; Okamoto, K. *Polyhedron* **2008**, *27*, 1432–1446.

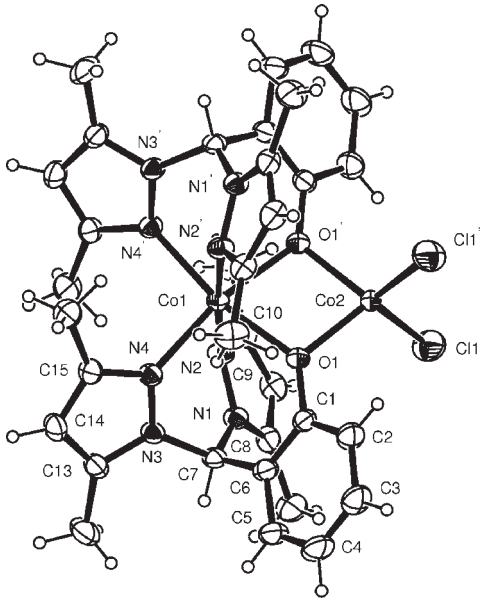

Figure 3. ORTEP view of complex **4** showing the thermal ellipsoids at 30% probability level.

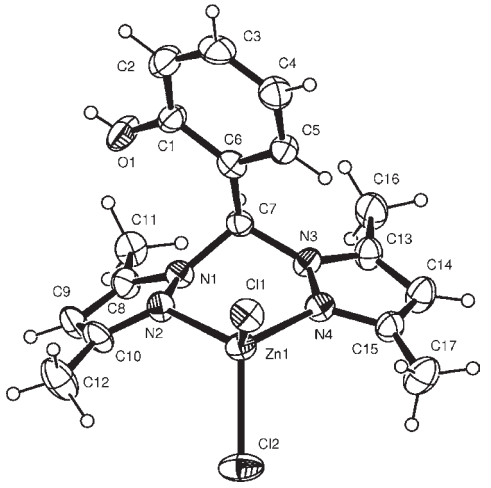

Figure 4. ORTEP view of complex **5** showing the thermal ellipsoids at 30% probability level.

NMR Spectroscopy of 1−6. Despite the paramagnetism of the metal center, the ^{1}H NMR spectra of cobalt(II) complexes exhibit relatively sharp but paramagnetically shifted resonances because of the favorable electronic spin relaxation times ($\tau_s \approx 10^{-11}$ s).[44] The ^{1}H NMR of (*L1*-H)$CoCl_2$ (**1**) exhibits well resolved signals in the range −20 to 45 ppm. The assignments of the ^{1}H NMR signals in Figure 6 have been made on the basis of the paramagnetic shift resulting from the proximity of the proton nuclei to the metal center, the integral ratios and T_1 values. The pattern of resonances is consistent with the presence of a plane of symmetry rendering equivalent the two pyrazole rings of the ligand. The outermost shifted signal at 42.53 ppm was assigned to the 5-methyl groups of the pyrazolyl rings whereas the 3-methyl groups of the same rings were found downfield shifted at −18.80 ppm,

(44) La Mar, G. N.; Horrocks, W.DeW.; Holm, R. H. *NMR of Paramagnetic Molecules; Principles and Applications*; Academic Press: New York, 1973.

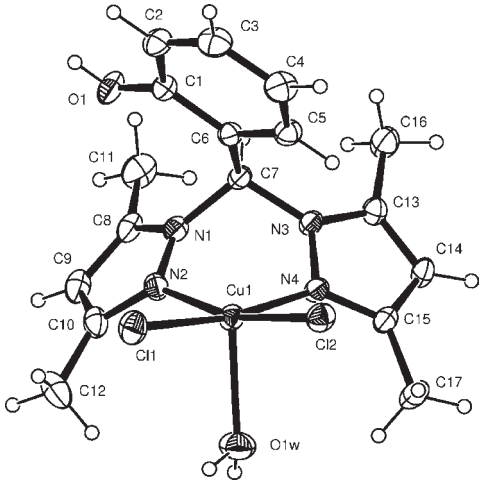

Figure 5. ORTEP view of complex **6** showing the thermal ellipsoids at 30% probability level.

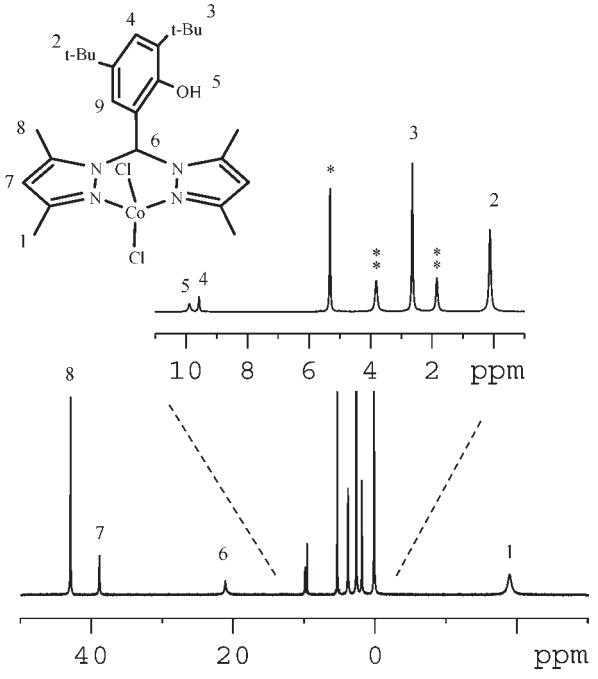

Figure 6. ^{1}H NMR spectrum (2 mM, CD_2Cl_2, 293 K) of **1**. See text for further discussion and assignments. The signal labeled with one star is due to the protio impurities of the deuterated solvent; the signals labeled with two stars are due to THF molecules clathrated in the crystalline compound.

probably as a result of different spin polarization effects in the pyrazolyl rings.[45] The methyl resonances of pyrazolyl rings have been distinguished by their different longitudinal relaxation times, as the 3-methyl groups are closer to the cobalt(II) ion and, hence, have T_1 values shorter than those of the 5-methyl protons. The signal of the phenol proton has been unambiguously identified at 9.88 ppm upon addition of D_2O which yields to the disappearance of this signal in the spectrum owing to a proton−deuterium exchange. The resonance of the H9 of the phenol group was not observed in the NMR spectrum, probably because of the extreme broadening of the signal due to the small distance between this

(45) Bertini, I.; Luchinat, C. *Coord. Chem. Rev.* **1996**, *150*, 29–75.

atom and the paramagnetic cobalt center (r_{H-Co} = 3.20 Å, based on the X-ray structure).

Assuming a predominant dipolar relaxation mechanism, the Co···H contact distance r should be proportional to $T_1^{1/6}$. Dipolar relaxation is defined by

$$T_1 = a \cdot r^6 \quad (1)$$

where r is the distance to the paramagnetic center, and a is a constant, which is equal for all the protons in the molecule. Equation 1 leads to a linear dependence between T_1 and r in a bilog plot, with the slope equal to 6. The T_1 dependence on the crystallographic distances for **1** is fairly accurate (see Supporting Information, Figure S2) and suggests that the solid state structure is retained in solution.

The ^{1}H NMR of $(L2)_2Co_2Cl_2$ (**4**) was previously reported by Higgs and Carrano.[17] They evidenced a partial dissociation of $[(L2)_2Co_2Cl_2]\cdot$MeCN in dichloromethane solution at 25 °C producing the monomeric sandwich species $(L2)_2$Co and solvated $CoCl_2$. While the ^{1}H NMR spectrum of the monomeric compound is completely within the −60 to +60 ppm range, the ^{1}H NMR spectrum of the dimer is spread out over the range −120 to +120 ppm.

The ^{1}H NMR spectra of the diamagnetic zinc complexes **2** and **5** are consistent with a high symmetric structure resulting from the κ^2-N,N coordination of the ligands to the metal center. The two pyrazolyl rings appeared equivalent showing that the structure is not rigid and the reorientation of the phenol ring is rapid on NMR time scale. The resonances of the pyrazol rings are generally downshifted when compared to those of the corresponding free ligands; for complex **2** the variation of chemical shifts ($\Delta\delta$) is in the range 0.25−0.41 ppm. This is consistent with a decrease in electron density due to coordination at the metal center. Also in these cases the solid state structures are retained in solution.

For mononuclear copper(II) complexes, ^{1}H NMR signals are generally not observed owing to the relatively long electronic relaxation time ($\tau_s \approx 10^{-9}$ s) for Cu^{2+} ion[44] which leads to line broadening. As matter of fact the ^{1}H NMR spectra of $(L3)CuCl_2$ (**3**) and of $(L2\text{-H})CuCl_2\cdot H_2O$ (**6**) show featureless broad resonances.

Investigation into the Formation of the *para*-Quinone Ligand *L3*. The aerobic oxidation of alkyl-phenols catalyzed by copper(II) salts, in the presence of nitrogen based compounds, is well established in the scientific literature.[46,47] Sun and co-workers reported the oxidation of 2,3,6-trimethylphenol to 2,3,6-trimethyl-1,4-benzoquinone[48] and proposed that this reaction is catalyzed by an oxotetracuprate cluster isolated from the reaction solution. Differently, Karlin and co-workers characterized an end-on bound superoxo copper(II) complex and demonstrated the catalytic properties of this species in the oxidation of 2,4,6-tri-*tert*-butylphenol to 2,6-di-*tert*-butyl-1,4-benzoquinone.[49] Very recently *para*-quinone-containing bis(pyrazol-1-yl)methane ligands were the subject of investigation by Wagner and co-workers.[50] These authors reported the efficient oxidative demethylation of *para*-dimethoxyphenyl-substituted bis(pyrazol-1-yl)methane ligands catalyzed by $[Ce(NH_4)_2(NO_3)_6]$.

To shed light on the factors governing the oxidation of *L1*-H, investigations into the formation of the *para*-quinone ligand to *L3* were carried out. At first, we developed a procedure that let us to easily identify the product outcome. The copper(II) complexes are paramagnetic and no resonance can be observed in the corresponding ^{1}H NMR spectrum. We thought to add an equivalent of *N*,*N*,*N*′,*N*′,*N*″-pentamethyl-diethylenetriamine (PMDETA) to an appropriate deuterated solution of the heteroscopionate copper complex for allowing the following substitution reaction:

$$(\text{Lig})CuCl_2 + \text{PMDETA} \rightarrow (\text{PMDETA})CuCl_2 + \text{Lig}$$

In the NMR spectrum of this mixture, since (PMDETA)$CuCl_2$ is a paramagnetic species, only the free ligand is detectable. To test this procedure, we prepared a THF-d_8 solution of $L3CuCl_2$ and we added 1 equiv of PMDETA into the NMR tube. In the corresponding ^{1}H NMR spectrum the pattern of resonances of *L3* was clearly observed. The aromatic protons on the *para*-quinone fragment give rise to a multiplet at 5.75 ppm and a doublet at 6.56 ppm. The resonance of the methine proton appears at 7.48 ppm. In the ^{13}C NMR spectrum the presence of the benzoquinone moiety is accounted by two low-field signals at 187.2 ppm and 185.6 ppm.

To determine whether the source of the oxygen atom in our oxidation reaction is dioxygen or water, we carried out the reaction between *L1*-H and $CuCl_2\cdot 2H_2O$ under nitrogen atmosphere in deaerated solvent. The product reaction was isolated and identified as $(L1\text{-H})CuCl_2$ (**7**) by means of elemental analysis, ESI-MS and ^{1}H NMR (Supporting Information, Figure S3) spectroscopy. Subsequently a known amount of **7** was dissolved in THF-d_8 ([10 mM]) and the corresponding solution was bubbled with dry oxygen for 2 h ([1 mM][51]). The corresponding ^{1}H NMR spectrum of this solution treated with 1 equiv of PMDETA clearly revealed the presence of *L3*. However, in solid state, **7** is quite stable: the exposure of the solid to air (two days) does not cause any morphologic change, the subsequent treatment of a solution of this sample with 1 equiv of PMDETA in $CDCl_3$ showed no evidence for the oxidation of *L1*-H to *L3*.

The kinetics of the oxidation reaction leading to **3** was investigated. To this end air was admitted to a mixture of *L1*-H and $CuCl_2\cdot 2H_2O$ in THF-d_8 (30 mM). The reaction was tracked by analyzing the product mixtures sampled from the reactor at certain reaction times. Each aliquot of this solution was treated with PMDETA and analyzed by ^{1}H NMR spectroscopy (Supporting Information, Figure S4). After an induction time of 30 min, in which hydrolysis of about 15 mol % of *L1*-H to 3,5-^{t}Bu$_2$-salicylaldehyde was observed, the oxidation of *L1*-H to *L3* started. After 2 h, *L1*-H was no longer present, and *L3* was the

(46) Punniyamurthy, T.; Rout, L. *Coord. Chem. Rev.* **2008**, *252*, 134–154.
(47) Lewis, E. A.; Tolman, W. B. *Chem. Rev.* **2004**, *104*, 1047–1076.
(48) Sun, H. J.; Harms, K.; Sundermeyer, J. *J. Am. Chem. Soc.* **2004**, *126*, 9550–9551.
(49) Maiti, D.; Fry, H. C.; Woertink, J. S.; Vance, M. A.; Solomon, E. I.; Karlin, K. D. *J. Am. Chem. Soc.* **2007**, *129*, 264–265.
(50) Blasberg, F.; Bats, J. W.; Bolta, M.; Lerner, H. W.; Wagner, M. *Inorg. Chem.* **2010**, *49*, 7435–7445.
(51) Battino, R.; Rettich, T. R.; Tominaga, T. *J. Phys. Chem. Ref. Data* **1983**, *12*, 163–178.

principal product (70%). The composition of the mixture do not change further with time.[52]

Finally we explored the role of the *tert*-butyl substituents of the phenol ring in the ligand oxidation. Two new ligands featuring only one *tert*-butyl group in *ortho* or *para* position, that is, (3-^{t}Bu-2-phenol)*bis*(3,5-Me_2-pyrazol-1-yl)methane (*L4*-H) and (5-^{t}Bu-2-phenol)*bis*(3,5-Me_2-pyrazol-1-yl)methane (*L5*-H) were properly synthesized and allowed to react with $CuCl_2 \cdot 2H_2O$ under the same experimental conditions employed for **3**. The reaction products (*L4*-H)$CuCl_2$ (**8**) and (*L5*-H)$CuCl_2$ (**9**) were isolated and characterized by elemental analysis and electrospray ionization mass spectroscopy (ESI-MS). In both cases no pieces of evidence of ligand oxidation were found. To corroborate these results, a known amount of both complexes was dissolved in $CDCl_3$ and treated with 1 equiv of PMDETA. In both cases the starting ligands *L4*-H and *L5*-H were observed in the ^{1}H NMR spectrum. We thus concluded that both *tert*-butyl groups in *ortho* and *para* positions of phenol group are required to ensure the oxidation of *L1*-H to *L3*.

Optical Properties and H_2S Detection by 1 and 2. H_2S is a colorless, flammable gas with a characteristic odor of rotten eggs and is considered one of the most dangerous environmental toxic and crude metabolic poisons.[53,54] It is more toxic than hydrogen cyanide and exposure to as little as 300 ppm in air for just 30 min can be fatal in humans.[55] In 2008 experimental evidence indicated that like carbon monoxide and nitric oxide, H_2S is an important signaling molecule in biology, and it may find a role in medicine.[56] Many natural sources produce H_2S, including volcanic gases, natural gas and coal reserves, sulfur springs, putrefying vegetable and animal matter. Several industrial processes also generate H_2S as a by-product. Easy and cheap monitoring of hydrogen sulfide is especially challenging. Cobalt and zinc ions are "borderline" soft Lewis acids[20] and therefore they should display a good affinity for H_2S. This prompted us to investigate the use of **1** and of the zinc analogue **2** in H_2S monitoring.

We first quoted the binding affinities of *L1*-H for Co(II) and Zn(II). Speciation of *L1*-H to cobalt(II) was determined by means of UV−vis spectroscopy. The absorption spectrum of a colorless THF solution of $CoCl_2 \cdot 6\ H_2O$ was monitored while adding increasing amounts of *L1*-H dissolved in THF (Figure 7). During the addition, the absorption peaks at 670 and 615 nm gradually increased together with a new band at 550 nm. The intensity of these peaks increased almost linearly until the [*L1*-H]/[Co^{2+}] molar ratio reached the value of one, corresponding to the formation of **1**. Meanwhile, additional absorption bands at 635 and 570 nm decreased to a limit value and were found slightly red-shifted. The presence of well-defined isosbestic points at 568, 591, 626, 643 nm indicated that only two species coexisted in the equilibrium. The Job's plot exhibited the inflection point at 0.5, which clearly indicates the formation of **1** in solution (see Supporting Information, Figure S5). An association constant K_a of $125 \pm 36 \times 10^3\ M^{-1}$ was obtained by a nonlinear least-squares fit[24] (see Supporting Information, Figure S6).

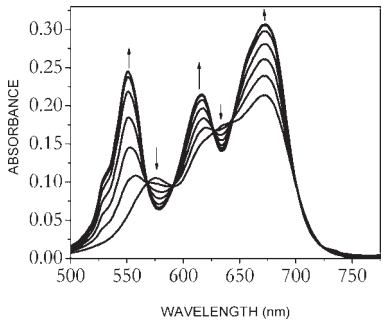

Figure 7. Absorption titration of $CoCl_2 \cdot 6H_2O$ with *L1*-H (RT, THF). [$CoCl_2 \cdot 6H_2O$] = 0.6 mM.

Speciation of *L1*-H/Zn^{2+} system had been previously evaluated by means of NMR spectroscopy.[7] The association constant was determined by fitting the plot of the variation of the chemical shift ($\Delta\delta$) observed for the 2-tBu resonance versus [Zn^{2+}]/[*L1*-H]. The K_a value was $7.8 \pm 0.3 \times 10^2\ M^{-1}$.[7] The lower K_a value found for Zn(II) can be ascribed to the lower acidic character of this cation compared to Co(II).

Both the complexes **1** and **2** are fluorescent and exhibit an emission band in the near UV region (around 320 nm). Interestingly the coordination to Co^{2+} and Zn^{2+} induces a fast enhancement of *L1*-H fluorescence in dichloromethane solution (switching ratio SR = 85% (**1**), 90% (**2**); Supporting Information, Figures S7 and S8), while a fast quenching was observed in THF solution (SR = 56% (**1**), 66% (**2**); Supporting Information, Figures S9 and S10). Thus the fluorescence of the *L1*-H ligand is turned-on by coordination to Zn^{2+} or Co^{2+} in dichloromethane, and turned-off in THF. This solvent dependent fluorescence intensity of *L1*-H was previously interpreted in the light of the different tendency to establish intra- or intermolecular hydrogen bonding (HB) interactions. Indeed, in THF solution the fluorescence intensity of *L1*-H resulted 30% higher than that registered in dichloromethane (Supporting Information, Figure S11).[7] Most likely, this finding could be the possible explanation for the different fluorescence trend observed for **1** and **2** in dichloromethane solutions and in THF solutions.

Then H_2S detection by **1** and **2** was investigated by means of fluorescence spectroscopy. Intriguingly, the bubbling of H_2S gas through a dichloromethane solution of **1** induces a fast and sizable enhancement of the fluorescence intensity, while it quenches the one of **2**, under the same experimental conditions (Figures 8 and 9). In other words, when H_2S is added to the solution the fluorescence of **1** "turns on" and that one of **2** "turns off". In dichloromethane (λ_{exc} = 290 nm) a fluorescence switching of 70% and 95% was found for **1** and **2**, respectively. This finding was corroborated adding increasing amounts of H_2S. In the case of **1** monitoring the fluorescence intensities a progressive enhancement was observed (Figure 8). Differently a progressive quenching was registered in the case of **2** (Figure 9). In both cases when plotting the fluorescence intensity values against the H_2S concentrations,

(52) Attemps to identify the other products of the reaction met with failure.

(53) Smith, R. P. *Am. Sci.* **2010**, *98*, 6–9.
(54) Smith, R. P. *Can. Med. Assoc. J.* **1978**, *118*, 775–776.
(55) Li, L.; Moore, P. K. *Biochem. Soc. Trans.* **2007**, *35*, 1138–1141.
(56) Yang, G.; Wu, L.; Jiang, B.; Yang, W.; Qi, J.; Cao, K.; Meng, Q.; Mustafa, A. K.; Mu, W.; Zhang, S.; Snyder, S. H.; Wang, R. *Science* **2008**, *322*, 587–590.

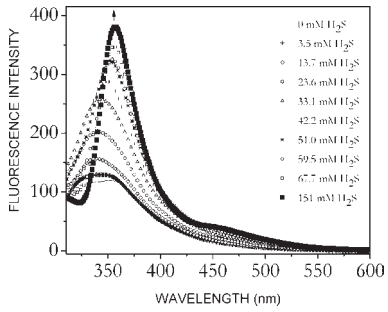

Figure 8. Emission spectra of **1** after addition of H_2S in the range of 0−151 mM (RT, CH_2Cl_2). [**1**] = 0.3 mM.

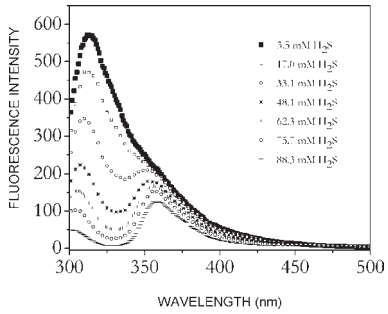

Figure 9. Emission spectra of **2** after addition of H_2S in the range of 3.5−88 mM (RT, CH_2Cl_2). [**2**] = 0.3 mM.

a trend could be found (Supporting Information, Figures S12 and S13).

When bubbling Ar through the solutions of **1** and **2** the initial fluorescence intensity values could not be restored.

We tried to assess the reasons why the fluorescence intensity of **1** and **2** changes upon H_2S addition. First we checked if **1** or **2** can coordinate H_2S, that is, if there is a minimum in the energy surface corresponding to the approach of the H_2S to the metal center. We performed a scan of the potential energy surface of the system composed of (*L1*-H)MCl_2 + H_2S for both cobalt and zinc. Constrained geometry optimizations at the BP86 level were performed by keeping fixed the M−H_2S distance at selected values in the range of 2.0−4.0 Å and relaxing all the other geometrical parameters. No minimum was observed in the corresponding curves (Supporting Information, Figure S14). This indicates that heteroscorpionate H_2S-complexes of both cobalt and zinc are not prone to form. The same conclusion was obtained by ^1H NMR spectroscopy when adding increasing amounts of H_2S to the solutions of **1** and **2**. In the case of **1**, the addition of increasing amounts of H_2S caused a slight shift of the proton NMR pattern. No resonances attributable to H_2S coordination were observed. When a large amount of H_2S was added to the NMR tube, a dark product precipitated and the pattern of the initial ligand begun to appear.

As observed above the fluorescence intensity of **1** is affected by the solvent, so the variation of fluorescence observed for **1** upon addition of H_2S could be ascribed to the change of the environment, that is, the non-covalent interactions that are necessarily established between the solute and the solvent. Indeed occurrence of non-covalent interactions as hydrogen-bonding is a well established tool of recognition in host−guest and solvent−solute systems.[57,58]

When H_2S was added to a CD_2Cl_2 solution of **2** the progressive hydrolysis of the coordinated ligand was observed. This was evidenced by the progressive increase of the signal at 11.37 ppm due to the aldehydic proton of 3,5-di-*tert*-butyl-salicylaldehyde (Supporting Information, Figure S15). Most likely the progressive quenching of the fluorescence observed for **2** upon addition of H_2S is due to the fact that when the starting ligand hydrolyzes it turns into species with lower fluorescence intensity. In view of these results, both **1** and **2** act as H_2S dosimeters, that is, irreversible devices, which progressively accumulate the dose, each time adding up the signal.[59,60]

All the H_2S dosimeters reported in the literature are substantially different than ours since they do not rely on coordination complexes. One of the first most efficient examples of H_2S dosimeters was reported at the end of the 1990s.[61] The method is based on trapping the H_2S in a solution with a chromophore. H_2S quantification is then made by monitoring the product.[61] A more sensitive variant of this type of methodology is the colorimetric tube.[62] Air is sucked through tubes which have been packed with silica gel impregnated with a silver-gelatin complex. In the present case the H_2S is detected by monitoring the formation of Ag_2S.[62] Chemically treated papers have been also widely used as H_2S dosimeters.[63] When these papers are exposed to hydrogen sulfide gas, a surface reaction on paper causes accumulation of the analyte, depending on the time of exposure and the concentration of hydrogen sulfide.[63]

Conclusion

In the present paper we reported on the synthesis and characterization of middle (Co^{II}) as well as late transition metal (Zn^{II}, Cu^{II}) complexes bearing phenol-substituted bis(pyrazolyl)methane ligands. At variance of the type of substituents in *ortho* and *para* position of the phenol moiety different coordination modes and reactivity were found. For the cobalt complexes, a mononuclear tetrahedral complex **1** or a dinuclear octahedral/tetrahedral complex **4** was obtained. In these complexes the heteroscorpionate ligand resulted κ^2- or κ^3-coordinated to the metal center, respectively. More interestingly, when reacting *L1*-H with copper, strong evidence indicated the aerobic oxidation of *L1*-H to the *para*-quinone derivative *L3* in which one *tert*-butyl group was replaced by an oxygen atom. In an effort to gain a better picture on the mechanism of the above oxidation reaction we repeated the reaction under an inert gas atmosphere in deaerated solvents, and we investigated ligands with different substitution patterns (*L1*-H, *L4*-H, *L5*-H). These experiments led to

(57) Kamlet, M. J.; Abboud, J. L.; Abraham, M. H.; Taft, R. W. *J. Org. Chem.* **1983**, *48*, 2877–2887.
(58) de Silva, A. P.; Gunaratne, H. Q.; Gunnlaugsson, T.; Huxley, A. J.; McCoy, C. P.; Rademacher, J. T.; Rice, T. E. *Chem. Rev.* **1997**, *97*, 1515–1566.
(59) Boiocchi, M.; Fabbrizzi, L.; Licchelli, M.; Sacchi, D.; Vazquez, M.; Zampa, C. *Chem. Commun.* **2003**, 1812–1813.
(60) Duong, T. Q.; Kim, J. S. *Chem. Rev.* **2010**, *110*, 6280–6301.
(61) Balasubramanian, N.; Kumar, B. S. M. *Analyst* **1990**, *115*, 859–863.
(62) Pal, T.; Ganguly, A.; Malty, D, S. *Analyst* **1986**, *111*, 691–693.
(63) Hayes, E. T.; Ataman, O. Y.; Karagozler, A. E.; Zhang, Y. L.; Hautman, D. P.; Emerich, R. T.; Ataman, A. G.; Zimmer, H.; Mark, H. B., Jr. *Microchem. J.* **1990**, *41*, 98–105.

the conclusion that the *L3* formation requires O_2 as oxidant and the presence of both *tert*-butyl substituents of *L1*-H.

The potential application of cobalt **1** and zinc **2** complexes as molecular recognition elements for H_2S was also explored. Addition of H_2S induced a modification of the fluorescence intensity in **1** or **2**. Interestingly, the presence of H_2S enhanced the fluorescence of **1** whereas it quenched that of **2**. In case of **1**, the variation of fluorescence intensity could be ascribed to the change of the environment, whereas, in case of **2**, it was originated from the hydrolysis reaction occurring upon addition of H_2S. The irreversibility of the process led us to the definition of **1** and **2** as dosimeters for H_2S, by comparison with literature nomenclature.[59,60] Design of dosimeters has recently emerged as an active research area of significant importance. Although the systems presented here have limited applications, our findings might be significant as a starting point for possible developments in the fast growing field of chemo-sensing and more specifically of the H_2S detection.

Acknowledgment. The authors thank Prof. Maurizio Licchelli of the Department of Chemistry (University of Pavia) for critically discussing the manuscript and Dr. Patrizia Iannece and Dr. Patrizia Oliva of the Department of Chemistry (University of Salerno) for their technical assistance.

Supporting Information Available: Figures S1−S15 (^{1}H NMR, absorption, fluorescence spectra and computational details) and X-ray crystallographic files (CIF). This material is available free of charge via the Internet at http://pubs.acs.org.